Article

LED light improved by an optical filter to visible solar-like light with high color rendering

Li-Siang Shen [1], Hsing-Yu Wu [2,3,4], Li-Jen Hsiao [2] and Chih-Hsuan Shih [1], Jin-Cherng Hsu [1,5,*]

[1] Department of Physics, Fu Jen Catholic University, No.510 Zhongzheng Rd., Xinzhuang Dist., New Taipei City 24205, Taiwan; 054326@mail.fju.edu.tw
[2] System Manufacturing Center, National Chung-Shan Institute of Science and Technology, New Taipei City 237209, Taiwan; andy810301@gmail.com
[3] Department of Electro-Optical Engineering, National Taipei University of Technology, Taipei 10608, Taiwan; andy810301@gmail.com
[4] Center for Astronomical Physics and Engineering, National Central University, Taipei 320317, Taiwan; andy810301@gmail.com
[5] Graduate Institute of Applied Science and Engineering, Fu Jen Catholic University, No. 510 Zhongzheng Rd., Xinzhuang Dist., New Taipei City 24205, Taiwan; 054326@mail.fju.edu.tw
* Correspondence: 054326@mail.fju.edu.tw; Tel.: 886-2-29053765

Abstract: A typical white-light light-emitting diode (LED) can achieve a sunlight-like spectral profile in the visible spectrum by means of using an optical filter, with an inverted transmission profile to the white LED, fabricated using a deposition coating process. The unfiltered white LED generates white light by mixing light emitted by a blue LED (450 nm) with emission from the yellow phosphorescence excited by the blue light and differs significantly from the characteristics of the full-spectrum natural light. In this study, the spectral characteristics of the filtered LED light can be improved to reach a general color rendering index value (R_a) of 95.6 at the D65.

Keywords: LED; solar-like light; optical coating; color rendering index; D65

1. Introduction

Since ancient times, human beings have always been most comfortable and adaptable during the day. Light is essential for our visual perception of our surrounding environment and affects both our physical and mental condition through our eyes and our skin. Daylight provides an excellent visual environment that benefits our physical and mental health through our eyes and skin by providing us with clear visual acuity and warmth, as well as in several other ways that do not necessarily involve image-forming effects. However, in certain times and places, for example, in an indoor setting during night time, the presence of daylight is absent, and as such, humankind has long since developed lighting sources with ever-increasing demands for comfort and safety, from burning wood, wax candles, light bulbs, and fluorescent lamps, to the current LED.

Color rendering is one of the essential characteristics of general lighting. It illustrates an object's natural chromaticity under a specific illumination source, for example, a white LED, for developments in general lighting. The color rendering index is the internationally recognized color rendering evaluation index [1]. The eight selected Munsell samples are first illuminated by a reference light source, then by the test light source, and then the color differences ΔE are calculated in the 1964 W*U*V* uniform color space [2]. The reference light source is Planck radiation with color correlated temperature (CCT) of 6500 K [3], with the light spectrum shown in Figure 1. The special color rendering index (CRI, R_i) of each color sample is given by

$$R_i = 100 - 4.6\,\Delta E_i \ (\ i = 1,\ldots,8), \quad (1)$$

and the score, the average of eight color samples, is the general color rendering index

$$R_a = \sum_{i=1}^{8} \frac{R_i}{8}. \quad (2)$$

The perfect color-rending light score is 100. Recently, most of the LEDs available in the market have shown an improvement in R_a up to values of about 80.

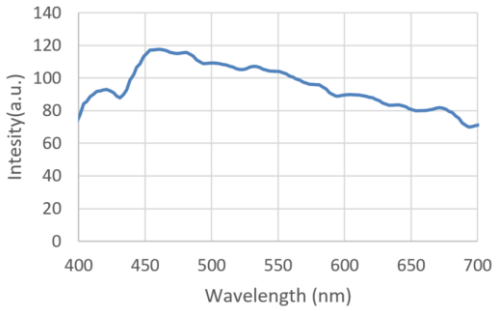

Figure 1. The light spectrum of D65.

D65 is used extensively in many visually demanding applications as a close substitute for natural daylight. With a corrected color temperature (CCT) of 6500 K, D65 is almost equivalent to sunlight during the day at noontime. Since recent years, LEDs have become the preferred light source for their high efficiency, color tunability, durability, long lifetime, energy efficiency, and environmental friendliness [4-6]. A typical white light LED uses a blue LED (mostly GaN or InGaN) with a central emission peak around 440 to 460 nm to excite a green/yellow phosphorescence and a red phosphorescence inside the sealing transparent silicone resin. The green phosphor has a central emission peak around 500 to 540 nm and the yellow phosphor around 545 to 595 nm. The emission from the blue LED and the green/yellow and red phosphorescence excitations then combine to form a pseudo white light emission, which is the reason for its name, white light LED.

This artificially synthesized white light often has a low color rendering index (R_a < 80) and a significantly higher CCT than 4000 K. To address this issue, some LED added more additional intermediate phosphorescence wavelengths and increased the intensity of the red phosphorescence. With the discovery of highly efficient red-emitting $CaAlSiN_3$:Eu^{2+}, $Sr_2Si_5N_8$:Eu^{2+}, K_2SiF_6:Mn^{4+}, or $SrLiAl_3N_4$:Eu^{2+} phosphors with multiple emission centers, the R_a can be improved to reach up to and exceed over 90 [7]. Moreover, developing novel phosphor in the white LED filled up the cyan gap between the blue and the yellow emission in the 470 to 500 nm region for higher quality general lighting [7,8]. In some patents and documentations, the high color rendering index is realized using a UV LED to stimulate multiple phosphor powder mixtures [9], forming multiple LED channels, then adding a neodymium oxide absorption filter to absorb the overly strong 580 nm emission peak [10]. All efforts enable humans to observe natural colored objects under the more commonly employed LED light sources.

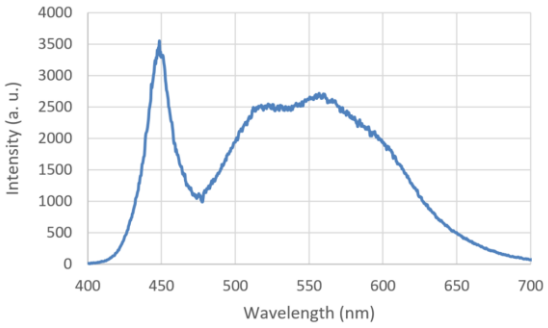

Figure 2. The measured emission spectrum of commercial phosphor-based white LED

Due to the energy-saving trait, LED light sources will likely see an even broader use in the future, in shops, restaurants, and everyday life in general. This research takes the approach of improving the most common commercially available white light LED, which has the emission spectrum as shown in Figure 2. By adding an optical filter that possesses

a transmission spectrum opposite to that of a typical white light LED, the intensity distribution of the emission radiation in the 450 to 650 nm range can be modified to become flat and in close resemblance to the high CRI D65.

2. Materials and Methods

The vacuum coating system is a 90-cm box coater (SGC-120SA-IAD, Showa Shinku CO.) equipped with a 10-kW electron beam gun and an end-Hall ion source (Mark II) made by Veeco Ion Tech. Inc. The coating materials are Al_2O_3, TiO_2, and SiO_2, respectively. A B270-glass substrate, 36 mm in diameter and 1 mm thick, is loaded onto a substrate holder. The vertical height extending from the circular hearth to the substrate is 75 cm. The horizontal distances from the beam-gun vaporization source to the substrate holder position is 30 cm. The holder is spun at a rotation rate of 30 rpm to ensure film distribution uniformity during the deposition. The off-axial source coating system is generally used to achieve coating uniformity. The vacuum chamber is pumped down to a base pressure lower than 5×10^{-6} Torr, and the substrate is heated to about 220 °C. Before the coating process, the substrate needs to be cleaned using an ion beam for ten minutes with a beam voltage of 120 V and a beam current of about 2.0 A. Oxygen and argon are introduced into the ion source as the working gas by setting the mass flow controllers to 5 and 10 sccm respectively. An automatic pressure controller is used to control the working pressure to about 8×10^{-5} Torr. After setting all of the deposition parameters above, this system can begin depositing the multilayer films onto the substrate.

The optical filter of this research is based on Southwell's design of optical notch filters with coupled wave theory [11]. Ideally, the refractive index of the multilayer stack should be a sine function of the film thickness. However, it is challenging to deposit the film in a sinusoidal refractive index using general electron gun evaporation due to the index variation in each film. In this research, we fabricated the symmetric stack notch filter in n fundamental periods, $(p/2\ q\ p/2)^n$, where p and q are odd multiples of quarter wavelength optical thickness with different refractive indices. The n value controls the transmittance at the central wavelength. The higher the n value, the lower the transmittance. The refractive index of the multilayer stack is a square wave function of the film stack thickness and is well within the fabrication capability of electron-gun deposition.

The full width of half maximum (FWHM), $2\Delta\lambda$, and the transmittance at the center wavelength (λ=450 nm) of the stack are related by Equation 3 [12]

$$2\Delta\lambda = \frac{4\lambda}{\pi} sin^{-1} \frac{n_M - n_L}{n_M + n_L}. \quad (3)$$

As indicated by Equation 3, the smaller the difference between n_M and n_L, the smaller the resultant FWHM will be. The two selected deposition materials are Al_2O_3 and SiO_2 at n_M =1.64 and n_L =1.45 at 450 nm wavelength, respectively, and the value of n is chosen to be 7 in this research. Moreover, the designed stack with Essential Macleod software (edited by Thin Film Center Inc., AZ, USA) p=3M and q=3L will be approximately 1/3 narrower than the stack created by p=M and q=L, as shown in Figure 3. The filter, therefore, was designed by the multilayer structure,

$$\text{Air / (1.5M 3L 1.5M)}^7 \text{ / Sub / (H'L')}^2 \text{ H / Air,} \quad (4)$$

where M is one quarter-wave optical thickness of the Al_2O_3, and L is one quarter-wave optical thickness of the SiO_2, respectively, on the top side of the B270 substrate (Sub). H' is one quarter-wave optical thickness of Ta_2O_5 ($n_{H'}$ =2.01 at 550 nm wavelength) and L' is one quarter-wave optical thickness of SiO_2 ($n_{L'}$ =1.445 at 550 nm wavelength) on the underside.

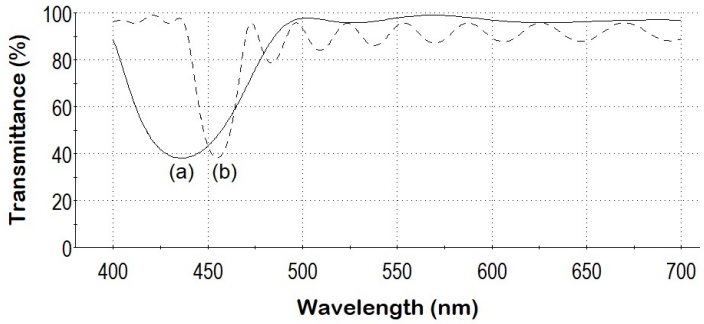

Figure 3. Notch filters, (a) $(0.5M\ L\ 0.5H)^7$ and (b) $(1.5M\ 3L\ 1.5H)^7$, are symmetric multilayer stack designed at 450-nm wavelength.

During the multilayer fabrication sequence, the deposition rate is controlled with a quartz monitor at 0.3 and 0.5 nm/sec for the SiO_2 and Al_2O_3, respectively. An optical thickness monitor is operated at the monitoring wavelength of 450 and 550 nm to control the deposited thickness on both sides of the substrate using the turning value method [13]. A spectrometer (USB 4000 System, Ocean Optics Inc., Florida, USA) is used to monitor the transmittance and the color temperature.

3. Results

3.1. Fabrication of filters

Figure 2 is the measured spectral profile of a typical commercially available white LED, which shows a narrow and intense peak at 450 nm, and a broader excited emission centered at 550 nm. To be balanced the non-uniformity, the measured spectra of D65 Ψ_{D65} and the LED Ψ_{LED} are first normalized to each of their highest intensity, respectively. The filter is then designed such that if Ψ_{LED} is passed through the filter with filter response Ψ_{filter}, the resultant filtered output would be Ψ_{D65}. That is,

$$\Psi_{Led}\ \Psi_{filter} = \Psi_{D65} \tag{5}$$

can be rearranged to get the following expression

$$\Psi_{filter} = \Psi_{D65} / \Psi_{Led}. \tag{6}$$

Figure 4 is a plot of the obtained target transmittance spectrum Ψ_{filter}. As can be clearly seen, the desired filter transmittance spectrum is almost an exact reverse of the LED spectrum. Ideally, the LED spectrum would pass through the multilayer filter film, and the two characteristic bands would be filtered each according to their distinct spectral intensity distribution, leaving the resultant filtered output spectrum in close resemblance to D65 natural light.

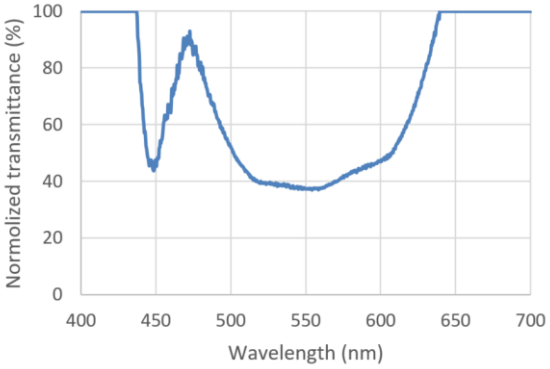

Figure 4. The target transmittance spectrum of the filter.

To be simplified both the filter design and the multilayer deposition process, two separate multilayer notch filters are deposited on two sides of the substrate to form the combined filter. Designing and fabricating a two-band notch filter with unequal notch widths on one side of the substrate is significantly more complex than separating the task

load to two sides of the substrate. The two multilayer designs can also control each of the two filtering characteristics independently during the deposition processes.

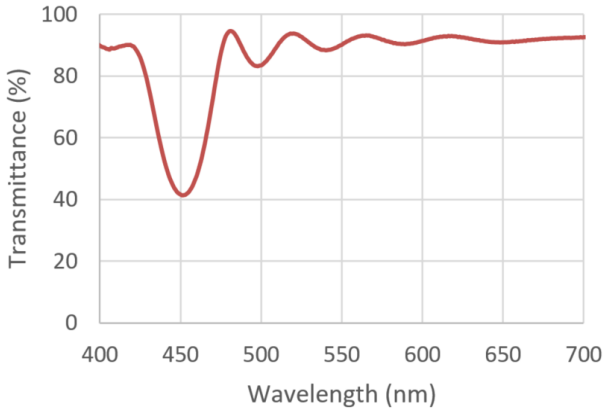

Figure 5. The spectrum of the notch multilayer on the first substrate.

Figure 3 (a) and (b) shows the design spectra of $(1.5M\ 3L\ 1.5M)^7$ and $(0.5M\ L\ 0.5H)^7$ notch filters, respectively. Although their design monitoring wavelengths are the same 450 nm, the wavelength of $(1.5M\ 3L\ 1.5M)^7$ notch filter's lowest transmittance is obviously less than 450 nm. During the coating process of the filter, the monitoring wavelength needs to be adjusted to locate the lowest transmittance wavelength at 450 nm. The notch spectrum has an FWHM of 33 nm and transmittance of 41.4 % at around 450 nm, as shown in Figure 5.

Table 1. Evaluations of FWHM and transmittance of the stack $(1.5M\ 3L\ 1.5M)^7$

	Simulated value [1]	**Experiment value**
FWHM (nm)	22.4	33.0
Transmittance (%)	38.2	41.4

[1] The value evaluated by the optical thin film.

Table 1 lists the notch FWHMs and the $(1.5M\ 3L\ 1.5H)^7$ stack transmittances. Both the software-simulated values and the actual measured values are listed. The software-simulated FWHM value of 22.4 nm differs significantly from the calculated FWHM value of 12.5 nm by Equation 3. The FWHM calculation using Equation 3 assumes constant refractive indices, which differs from the actual case since the film's refractive index values of the optical mediums are functions of the wavelength. Generally, the shorter the wavelength is in the visible spectral range, the higher the refractive index. The FWHM evaluated by the thin film software, not disregarding the dispersion property of the films, is larger than the FWHM evaluated by Equation 3. The film stack transmittances with seven fundamental periods (i.e., n=7) are 38.2% for the software simulation and 41.4% for the experiment value. The FWHM value by experimental measurement is larger than the simulated value, likely due to the non-uniformness in the distribution of the refractive index of the deposited films. Figure 5 shows the spectrum of the first fabricated filter, a multilayer notch filter, which reduces the spectral intensity of a specific wavelength band in the range between 440 to 460 nm, and the magnitude is dependent on the intensity peak of the 450-nm light of LED.

As shown in Figure 2, the FWHM of the yellow phosphorescence from the excitation of the 450 nm light ranges between 490 to 610 nm. The second multilayer deposited on the other side of the substrate has a broader reflection spectrum centered around 550 nm resulting from the significant refractive index difference between $n_{H'}$ and $n_{L'}$ of Equation (4). Increasing the number of the H'L' layer pairs of Equation (4) can independently decrease the emission of the excess yellow phosphorescence in the spectrum, with the lowest transmittance centered at 550 nm, as shown in Figure 4. Also, the transmission

spectrum of the H'L' layer pair exhibits a high transmission at 450 nm, as shown in Figure 6.

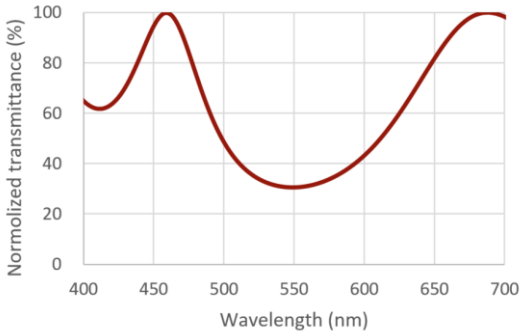

Figure 6. The broad spectrum on the second surface of the substrate.

3.2. Optical properties of the modified light module

Figure 7 is a plot of the transmission spectra in the visible spectrum of three of the combined filters. The R_a values of the three assemblies are 93.5, 92.4, and 95.8, respectively. To integrate the filter onto the LED lamp, simply place the filter in front of the LED, as shown in the configuration in Figure 8.

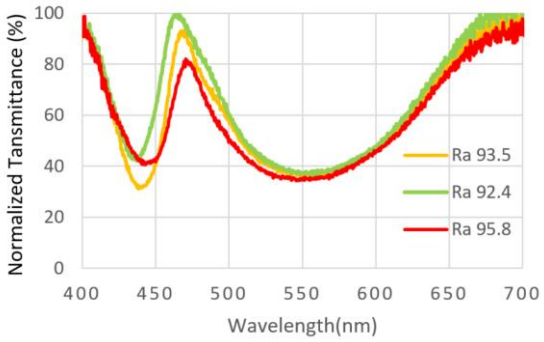

Figure 7. The spectra of the three combined filters

Figure 8. A 7-watt LED cup light covered with a combined filter.

The LED module in Figure 8, by itself, consists of an array of blue LEDs with a narrow emission peak centered around 450 nm as the excitation source, a green/yellow and red phosphorescence layer, to be excited by the emission from the blue LED. Figure 9 is a plot of the emission spectrum of a typical unfiltered white LED, the emission spectra of the LED after passing through the three fabricated filter samples, and the emission spectrum of D65 as a reference. The fabricated filter samples reduce the blue 450 nm emission peak and the excess phosphorescence centered around 550 nm, though the cyan gap between the blue and yellow emission around the 470 to 500 nm region still instigates challenges in enhancing the overall color reproduction. The fabricated filters only slightly dampen

the intensity around the 475 nm region. At the D65 color temperature, the *Ra* values of the three filtered LEDs are 93.5, 92.4, and 95.8, respectively, with the 95.8 *Ra* spectrum matching closer to the D65 spectrum than the 92.4 *Ra* and the 93.5 *Ra* spectrum.

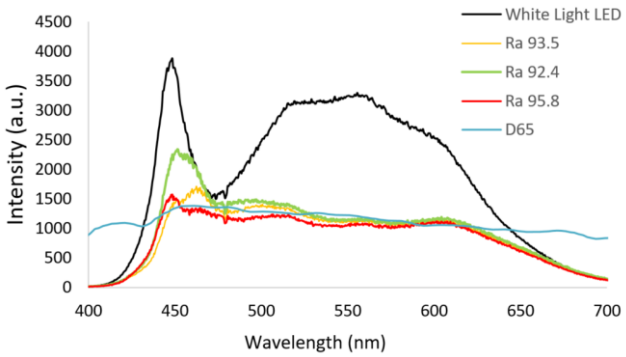

Figure 9. The spectra of the white light LED module, the LED module equipped with the three combined filters, and D65 light.

Figure 10 is a diagram showing the hue of three wooden boards under three different illumination conditions. Figure 10 (a) is illuminated under a 3200 K white LED, Figure 10 (b) is illuminated under a white LED with the filter integrated, and Figure 10 (c) is illuminated with a 6000 K white LED. The boards are painted in the gray 5N level to minimize the interference to the hue of the painted boards under the three illumination conditions. Under illumination by the 3200 K white LED and the 6000 K white LED, the color appears slightly unnatural, with the 3200 K LED slightly over accentuating the yellow in the overall tint and the 6000 K LED exhibiting an uncomfortable glare, respectively. With a white LED, the blue 450 nm LED serves both as the excitation source to excite a yellow (and possibly also green and red) phosphorescence and to combine with it to form a "white" light [10]. By the filter with the transmission spectrum in the shape of the inverted spectrum of a typical white LED, the spectral intensity in the overly prominent wavelength bands can reduce to provide a white illumination to objects while retaining their original color. After the filter, the overall output power of the LED can be observed to be reduced to almost half of that of the original unfiltered white LED, though as Žukauskas et al. pointed out, more natural-looking light with better color saturation and more preferred by most people often appears duller and mellower [14]. Also, according to the study of Babak Zandi et al., the change in human pupil diameter reacts more vital towards stimuli at longer wavelengths in the visible spectrum; however, with shorter wavelengths towards the blue end of the spectrum, there is little to no change at all. The means that under the same luminosity, the same human-perceived brightness, and therefore similar eye pupil diameter, light from typical unfiltered white LED contains a much larger portion of the higher energy 450-nm blue light, which may cause damage to the retina inside the human eye, since the human-pupil diameter is less responsive towards blue light. Other than inducing photoreceptor damage, excessive exposure to blue light may also affect a person's physiological functions as well, though it is worth noting that blue light can be potentially used in applications regarding the treatment of certain circadian disorders and sleep-related dysfunctions [15]. Nevertheless, minimizing the risks related to the spectral output of LED-based light sources associated with prolonged exposure to blue light is essential.

(a) (b) (c)

Figure 10. The LED light source (a) 3200-K LED light source, (b) modified LED light source, and (c) 6000-K LED light source to emit three light colors in a three-grid wooden box painted in the gray 5N level, and their R_a values are about 80 at 2800 K color temperature, 95.6 at 6500 K, and 80 at 6000 K, respectively.

4. Discussion

An optical filter with the inverted spectrum of a white LED is designed and fabricated in this study. The fabricated filter is placed in front of a commercially available 6000 K white LED source. It can be tested to increase the color rendering index of the white LED from 80 to 95.6 at the D65 color temperature. The filter is fabricated by coating two multilayer notch filters, each on one side of the filter substrate, through deposition processes. At high incident angles, the resultant emission can be observed to undergo a blue shift due to the angular dependency of the filter spectrum. In future developments, this issue may be mitigated by using curved substrates in the deposition process to decrease the angle of incidence. For the scope of this study, however, this issue is solved simply by applying a small aperture to block out the illumination at large angles, as can be observed in Figure 10 by the small circular area of lighting on the painted boards.

Currently, the most commonly available white LEDs use a combination of blue LEDs and complementary yellow phosphor as the working mechanism. This method has the advantage of structural simplicity and high emission efficiency and has become the mainstream method of producing white light using LEDs. However, on the other hand, this kind of white light LED results in higher irradiance towards the shorter wavelengths, more specifically in the blue wavelength region ranging from 450 to 500 nm. This study addresses the issue by designing and fabricating optical filters consisting of multilayer films to be coated onto both sides of the substrate to act as a limiter. The multilayer is designed to a specific spectral response through spectrogram analysis of the white light LED spectrum, such that smooth resultant illumination spectral intensity profile forms in the visible range between 400 and 700 nm. In the three filter test samples fabricated, the spectrum of the filtered white LED can reach as high as 95.6 R_a at the D65 color temperature. Objects under illumination by this filtered white LED can better retain their original natural colors and appearances. The lighting of this kind has high potential in applications involving presenting objects while preserving their actual colors and textures, such as artwork and presentation lightings, retaining the market and artistic value of the artwork with high CRI illumination. Note that for the filter to function properly and increase the R_a value, the color temperature of the selected unfiltered white LED must be higher than 6000 K because low color temperature LEDs lack the characteristic 450 nm peak. Moreover, to further increase the R_a value, as can be deducted from observing Figure 9, one possible way is to add the lights of 405 and 680-nm LEDs to the mixture light [16].

Using the multilayer filters has many advantages: Fabrication ease, well-studied and well-documented design logic, and relatively low fabrication cost. The size of the LED

determines the required filter and substrate size, and direct attachment to the hot LED source is also possible due to the generally high heat resistance of the substrate and multilayer materials. The phosphorescence effect may also be simultaneously improved due to the increased back reflection of the 450 nm blue light. This filtering method is safer and less harmful than using UV LEDs and UV-specific phosphors to produce high CRI lighting and better structural simplicity than multichannel LEDs. By the same principle and process, this filtering method may also increase the already high *Ra* of an existing LED source to reach 100 R_a potentially.

5. Conclusions

In this study, an optical filter with a transmission profile in the shape of the inverted spectrum of a typical white LED is designed and fabricated. The filter is placed in front of a commercially available 6000 K white light LED source and can be observed to increase the R_a value from 80 to 95.6 at the D65 color temperature. The filter is fabricated by coating two multilayer notch filters each on one side of the substrate using deposition processes. The filter can be placed directly in front of the LED chip or an existing LED module.

Author Contributions: Conceptualization, J.C.; methodology, J.C. and L.S.; software, L.S.; validation, L.S.; formal analysis, H.Y.; investigation, H.Y.; resources, J.C. and H.Y.; data curation, C.H.; writing—original draft preparation, J.C. and L.J.; writing—review and editing, J.C. and L.J.; supervision, J.C.; project administration, C.H.; funding acquisition, J.C. and H.Y.

Funding: This research was funded by the Ministry of Science and Technology of Taiwan, grant number MOST 106-2221-E-030-007-MY3 and MOST 106-2112-M-030-001.

Institutional Review Board Statement: Not applicable.

Informed Consent Statement: Not applicable.

Data Availability Statement: The data is included in the article.

Acknowledgments: The authors gratefully acknowledge Tzu-Ning Chen for his optical coating technical support.

Conflicts of Interest: The authors declare no conflict of interest.

References

1. Ohno, Y. Spectral design considerations for white LED color rendering. *Opt. Eng*. **2005**, 44, 111302.
2. Soltic, S.; Chalmers, A.N., Influence of peak wavelengths on properties of mixed-LED white-light sources. *Adv. Optoelectron.* **2010**, 2010.
3. Schanda, J. Colorimetry: Understanding the CIE System; A John Wiley& Sons, Inc.: New Jersey, USA, **2007**; 25–78.
4. Pust, P.; Schmidt, P.J.; Schnick, W. A revolution in lighting. *Nat. Mater.* **2015**,14, 454–458.
5. Pimputkar, S.; Speck, J.S.; DenBaars, S.P.; Nakamura, S. Prospects for LED lighting. *Nat. Photon.* **2009**, 3, 180–182.
6. Schubert, E.F.; Kim, J.K. Solid-state light sources getting smart. *Science* **2005**, 308, 1274-1278.
7. Zhao, M.; Liao, H.; Molokeev, M.S.; Zhou, Y.; Zhang, Q.; Liu, Q.; Xia, Z. Emerging ultra-narrow-band cyan-emitting phosphor for white LEDs with enhanced color rendition. *Light Sci. Appl.* **2019**, 8, 1-9.
8. Strobel, P.; de Boer, T.; Weiler, V.; Schmidt, P.J.; Moewes, A.; Schnick, W. Luminescence of an oxonitridoberyllate: a study of narrow-band cyan-emitting $Sr[Be_6ON_4]: Eu^{2+}$. *Chem. Mater.* **2018**, 30, 3122-3130.
9. Zhang, F.; Xu, H.; Wang, Z. Optimizing spectral compositions of multichannel LED light sources by IES color fidelity index and luminous efficacy of radiation. *App. Opt.* **2017**, 56, 1962-1971.
10. Matsubayashi, Y.; Yagi, H.; Shimizu, M.; Manabe, Y.; Motoya, A.; Matsuo, K.; Mori, T. LED lamp, LED illumination device, and LED module. U.S. Patent No 9,062,851, **2015**.
11. Southwell, W.H. Spectral response calculations of rugate filters using coupled-wave theory. *J. Opt. Soc. Am.* **1988**, A.5, 1558-1564.
12. Macleod, H.A. *Thin-film optical filters*, 4th ed.; CRC Press: New York, USA, **2010**; p.222.
13. Macleod, H.A. Turning value monitoring of narrow-band all-dielectric thin-film optical filters. *Optica Acta: Int. J. Opt.* **1972**, 19, 1-28.
14. Žukauskas, A.; Vaicekauskas, R.; Vitta, P.; Tuzikas, A.; Petrulis, A.; Shur, M. Color rendition engine. *Opt. Express* **2012**, 20, 5356-5367.
15. Zandi, B.; Klabes, J.; Khanh, T. Q. Prediction accuracy of L-and M-cone based human pupil light models. *Sci. Rep.* **2020**, 10, 1-14.

16. Baek, S.; Kim, S.; Noh, J.Y.; Heo, J.H.; Im, S. H.; Hong, K.H.; Kim, S.W. Development of mixed-cation $Cs_xRb_{1-x}PbX_3$ perovskite quantum dots and their full-color film with high stability and wide color gamut. *Adv. Opt. Mater.* **2018**, 6, 1800295.